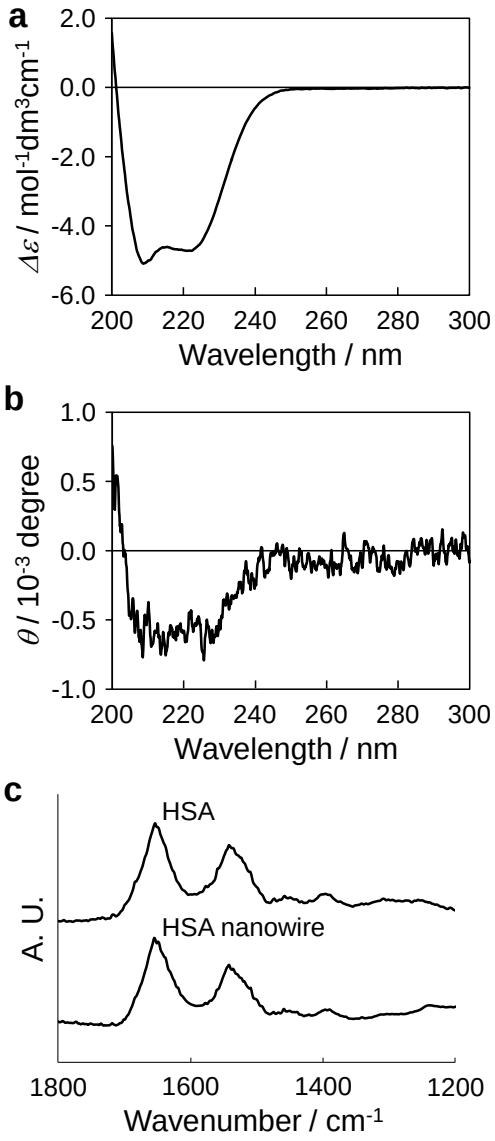

Supplementary Figure 1. Structural analysis of HSA nanowires.

Circular dichroism of (a) HSA and (b) HSA nanowires in PBS. (c) FTIR-ATR spectra of the HSA and HSA nanowires on Si wafer in the region of 1800–1200 cm^{-1}.

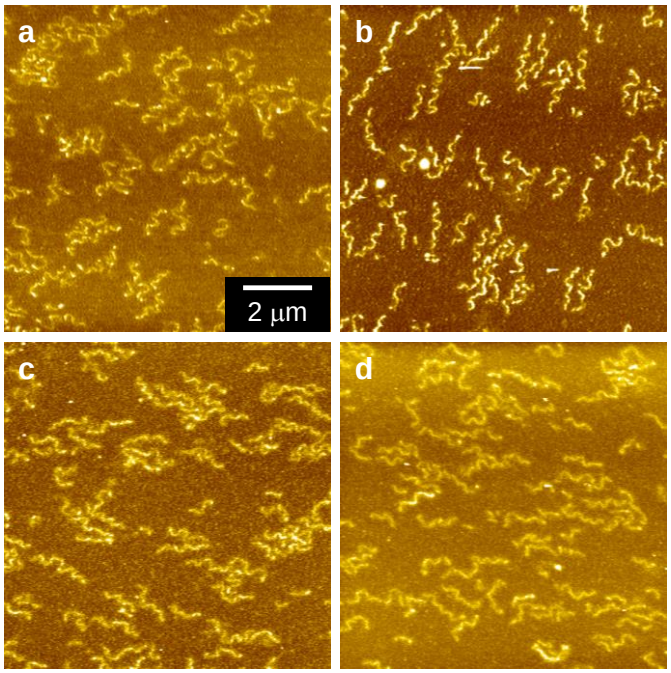

Supplementary Figure 2. Stability of HSA nanowires.

AFM images of HAS nanowires (a) prepared freshly and (b) after three months in the atmosphere, followed by immersing into PBS for (c) 6 hours and (d) 12 hours at 25 ^{o}C.

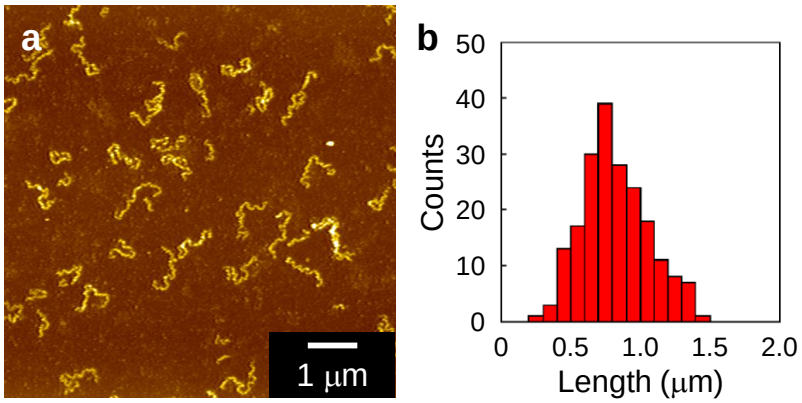

Supplementary Figure 3. Effect of the thickness of the film on the fabrication of HSA nanowires with high aspect ratio.

(a) AFM image and (b) length distribution of the HSA nanowires formed by irradiation of a 1.0 μm-thick HSA spin-coated film with a 490 MeV $^{192}Os^{30+}$ ion beam at a fluence of 1.0×10^{8} ions cm^{-2}.

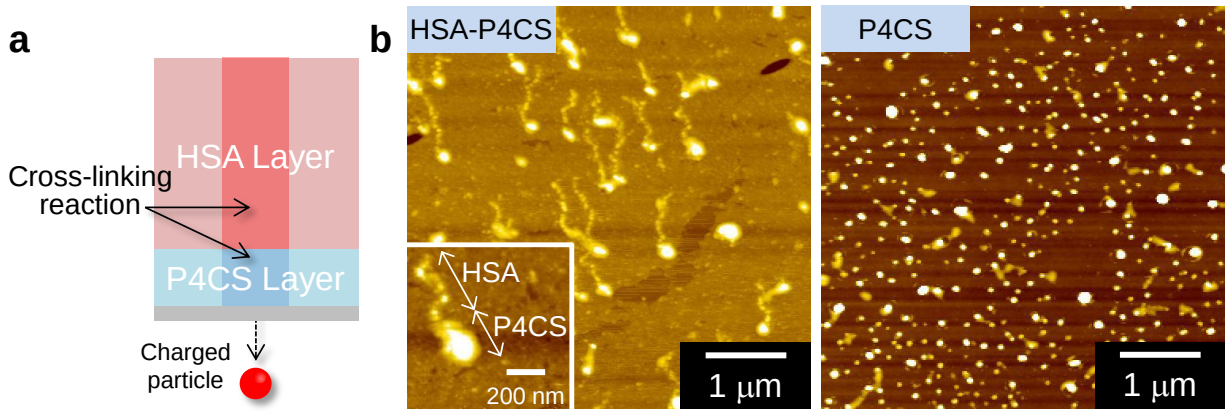

Supplementary Figure 4. Fabrication of HSA-P4CS connected nanowires.

(a) Schematic image showing the formation of HSA-poly(4-chlorostyrene) (P4CS) connected nanowires by SPNT from an HSA (upper) and P4CS (lower) bilayer film. (b, left) AFM image of the HSA-P4CS connected nanowires fabricated by exposure to a 490 MeV $^{192}Os^{30+}$ ion beam at a fluence of 1.0×10^{8} ions cm^{-2}. (b, right) AFM image of the P4CS nanodots formed by irradiation of a 90 nm-thick P4CS spin-coated film with a 490 MeV $^{192}Os^{30+}$ ion beam at a fluence of 1.0×10^{9} ions cm^{-2}.